JTTEE5 23:447–455
DOI: 10.1007/s11666-013-0010-0
1059-9630/$19.00 © ASM International

Fabricating Aluminum Bronze Rotating Band for Large-Caliber Projectiles by High Velocity Arc Spraying

Bin Wu, Ling-hui Fang, Xiao-lei Chen, Zhi-qiang Zou, Xu-hua Yu, and Gang Chen

(Submitted May 20, 2013; in revised form August 17, 2013)

The necessity of finding new rotating band materials and developing corresponding joining technologies for large-caliber projectiles has been revealed by the recent increase in the ballistic performance of high loads. In this paper, aluminum bronze coatings were fabricated by the high velocity arc spraying (HVAS) technique. Microstructure and microhardness of the prepared coatings were investigated. Ring-on-disk dry sliding wear tests were conducted in an ambient condition to examine the tribological behavior of the coatings. Quasi-static engraving processes of rotating bands made of as-sprayed aluminum bronze coating and bulk copper were studied using rate-controlled push test methodology on an MTS 810 Material Testing System. The results show that the as-sprayed aluminum bronze coatings have a dense microstructure with porosity of about 1.6%. Meanwhile, the as-sprayed coating presents a higher microhardness than pure copper. The friction coefficient of coatings is about 0.2-0.3 in the steady state. Tribological mechanisms of the as-sprayed coatings were discussed. The engraving test results show that the aluminum bronze rotating band presents high bonding strength and good plasticity. The HVAS aluminum bronze coating should be a possible substitute for the state-of-the-art copper rotating band.

Keywords aluminum bronze, high velocity arc spraying, large-caliber projectile, rotating band

1. Introduction

The field of ballistics can be broadly classified into three major disciplines: interior ballistics, exterior ballistics, and terminal ballistics. Interior ballistics deals with the interaction of the gun, projectile, and propelling charge before emergence of the projectile from the muzzle of the gun (Fig. 1). Separate loading ammunition consists of the projectile, which is loaded first into the weapon, the propellant charge, loaded next, and finally the primer and igniter, loaded last.

A rotating band is composed of a soft metal that is sealed securely to the projectile body. Before the projectile travels down the bore, the rotating band must be swagged to the bore diameter and engraved by the rifling. Once the rotating band has been fully engraved, the rifled bore acts to impart spin to the projectile. The primary functions of the rotating band of separate loading ammunition for a large-caliber gun can be summarized as follows: (1) to seal the bore to prevent leakage of the generated propellant gas around the projectile; (2) to position and center the rear end of the projectile; and (3) to help transmit a rotation to the projectile. Therefore, the rotating band greatly affects muzzle velocity, range, accuracy, and gun barrel life.

Montgomery (Ref 1-5) investigated the interaction of copper-containing rotating band metal and gun bores in the environment present in a gun tube. It was found from examination of recovered projectiles and fired cannon tubes that melt lubrication of projectiles sliding on a gun bore has really occurred, which means that the rotating band material must be high melting one. Matsuyama (Ref 6) proposed a melting wear theory and established a practical selection method of slider materials, such as red brass, Al-bronze, and brass. Theoretical and experimental studies were performed on the wear mechanism of 105- and 155-mm artillery projectile rotating band by Lisov (Ref 7).

Traditionally, the rotating band is made of commercially pure copper, copper alloy, or plastic. For small- and medium-caliber projectiles, the rotating bands are made of commercially pure copper or gilding metal. Large-caliber projectile bands are made of brass, cupro-nickel alloy, or soft iron. However, the rotating band is identified as the weakest link in the gun-projectile-charge system due to a recent increase in the ballistic performance of high loads. Schupfer et al. (Ref 8) investigated three alternative materials, nickel, titanium, and carbon fiber-reinforced composite (CFC), as possible substitutions for copper rotating bands. Corresponding processes for joining the band on the projectile were also developed due to the physical properties of these three materials. The nickel rotating band was fixed to the thin-wall carrier projectile by a specially designed welding process on a welding machine. It was impossible to connect the titanium with steel by welding because of the tendency of forming

Bin Wu, Ling-hui Fang, Xiao-lei Chen, Zhi-qiang Zou, Xu-hua Yu, and **Gang Chen**, New Star Research Institute of Applied Technology in Hefei, Anhui 230031, P. R. China. Contact e-mail: mewubin@tom.com.

intermetallic phases. The titanium band was statically pressed onto the projectile by means of a radial press. A thermal shrinkage process was developed for joining the CFC rotating band on the projectile.

It is of great necessity that new rotating band materials should be found and corresponding joining technologies be developed for large-caliber projectiles due to actual problems induced by use of high energy ammunition. Copper is a widely used metal whose properties can be enhanced by alloying. Some copper-based alloys, such as Cu-Al, Cu-Zn, and Cu-Al-Fe, are used for industrial applications because they are reasonably good load-bearing materials with high wear and corrosion resistance. Aluminum bronzes are copper-based alloys typically containing about 5-12% by weight aluminum and optionally small amounts of other elements such as iron, nickel, zinc, manganese, and tin with the balance being copper. Thermal spray technology is one of the possible solutions to fabricate aluminum bronze coating due to the lower cost of production and the ability to produce coatings with complex shapes. Thermally sprayed aluminum bronze coating is widely used in many practical applications. Akdogan et al. (Ref 9) investigated the surface fatigue of Al-bronze coating in unlubricated rolling/sliding contact. The high temperature oxidation behavior of arc-sprayed aluminum bronze coatings on steel substrate was studied by Zhang et al. (Ref 10). Alam et al. (Ref 11) studied the tribological characteristics of low pressure plasma-sprayed aluminum bronze coatings against a steel ball. Tan et al. (Ref 12) investigated the slurry erosion behavior of high velocity oxy-fuel (HVOF)-sprayed aluminum bronze coatings. Aluminum bronze-alumina composite coatings were prepared on mild steel substrate using conventional plasma spray and cold spray (CS) techniques by Miguel et al. (Ref 13).

In the present research, an attempt has been made to assess the potential of the coatings of aluminum bronzes, synthesized by high velocity arc spraying (HVAS), as rotating bands for large-caliber projectiles. The coating structure, microhardness, and mechanical and tribological performance were characterized. Quasi-static engraving processes of rotating bands made of as-sprayed aluminum bronze coating and bulk copper were studied using rate-controlled push test methodology.

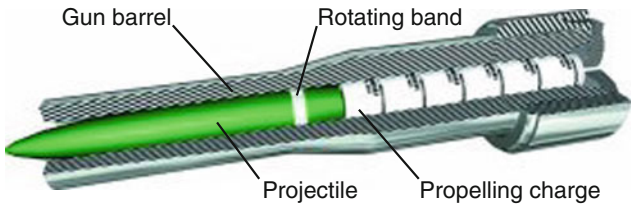

Fig. 1 A schematic of gun-projectile-charge combination

2. Experimental

2.1 Materials and Equipment

The experimental setup of fabricating the rotating band is shown in Fig. 2. Mild steel of 0.45% carbon steel was chosen as the substrate for coating deposition. Two kinds of specimens were deposited. One is a hollow cylinder with outer diameter 73 mm, inner diameter 63 mm, and length 200 mm and the other is a plate of 200 mm × 200 mm × 4 mm dimension. Prior to arc spraying, the substrate was degreased with acetone, dried in air, and then grit blasted. The spray material was self-made aluminum bronze wire of 1.6 mm diameter (chemical composition listed in Table 1). The morphology of the aluminum bronze wire is shown in Fig. 3. The final coating thickness on the plate was maintained within the range of 0.5 ± 0.05 mm and that of the hollow cylinder was 3 ± 0.1 mm. The arc spray was carried out using a CMD-AS 3000 electric wire arc spray machine consisting of a power supply, a control unit, and a self-designed HAS-2 HVAS gun. The hollow cylinder was rotated on a rotary table at a speed of 60 rpm. The spray parameters (voltage, current, air pressure, and spray distance) of the electric arc spray process were optimized using the Taguchi method (Ref 14) and are shown in Table 2.

2.2 Coating Characterization

The microstructures of the coatings were observed using a Philips Quant 200 SEM equipped with an Energy Dispersive x-ray (EDX) analysis apparatus. EDX microanalyses on the

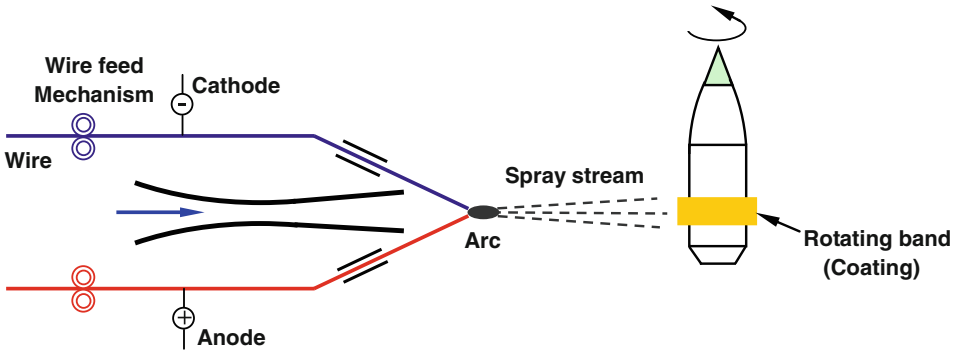

Fig. 2 Schematic view of the electric wire arc spray process setup

Table 1 Chemical Composition of Aluminum Bronze Wire (wt.%)

Al	Si	Sn	Mn	Zn	Ni	Pb	P	Others	Cu
8.0-10.0	0.1	0.1	0.5	1.0	0.5	0.01	0.01	1.7	Balance

Fig. 3 Photo of the aluminum bronze wire

Table 2 Optimized Electric Arc Spraying Parameters

Parameter	Setting
Arc voltage	30 V
Arc current	180 A
Air pressure	0.7 MPa

cross section of coatings have been conducted to determine the weight fraction of each element in the coating. The EDX analysis has been conducted at least five times at a low magnification (150×) in different zones for each coating, and the results were considered to be representative. An estimation of the porosity of the coatings has been conducted by image analysis; at least 10 SEM images (which nearly cover the whole area of the cross section of the coatings) of low magnification (150×) have been used to make a statistic on coating porosities. A Vickers microhardness tester HXD-1000 at a load of 100 g was used to determine the hardness of the cross section of all coatings produced. Indentation parameters were set as 15-s loading time and average thickness was derived from five measurements. All the measured Vickers hardness values are mean of 10 indentations. Dry sliding wear tests were performed on an MMG-10 Ring-On-Disk (ROD) tribometer (as schematically represented in Fig. 4) under ambient environment (temperature: ~25 °C; humidity: 40-50%). During the test, the testing specimen (disk) was stationary and the counterpart (ring) was rotating. The coatings were subjected to a 15-min test during which a ring of dimension outer diameter 28 mm, inner diameter 22 mm, and height 30 mm was used as the counterface material at speeds of 60 and 180 rpm. Loads of 70 and 110 kg were applied normal to the coatings. As we know, friction

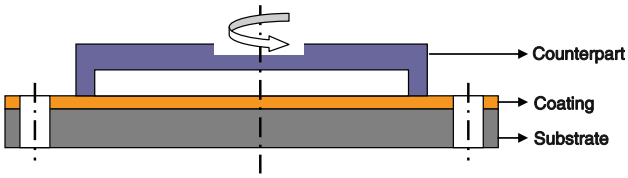

Fig. 4 Schematic representation of tribological test apparatus

between the rotating band and gun bore surface from firing a low-charge round is slight, whereas that of a high-charge round is severe. Therefore, in the present tribological tests, low rotational speed and low load (60 rpm and 700 N) simulate the low-charge zone; high rotational speed and high load (180 rpm and 1100 N) resemble the high-charge zone. The friction force was measured by a sensor with the accuracy of 3% F.S. and dynamically recorded into a computer. The friction coefficient was computed when the friction force was divided by the applied load. Each specimen was weighed before and after the test, using a BT22S electronic scale with an accuracy of 0.01 g. The surface morphologies of the worn tracks were observed using SEM.

2.3 Quasi-static Engraving of Rotating Band

To evaluate the plasticity and shearing strength of the as-sprayed aluminum bronze rotating band, quasi-static experiments were conducted on an MTS 810 Material Testing System, as shown in Fig. 5. A simulated short gun barrel made of CrNiMo steel was prepared for push testing, for which the land diameter, groove diameter, and outer diameter were 75.5, 77.2, and 100 mm, respectively. To simplify the manufacturing process and subsequent analyses, linear rifling, namely, the rifling profile without a twist, was adopted in the push tests. The length of the barrel was 230 mm with rifling 60 mm long. The width of the land and groove was 2.10 and 5.38 mm, respectively. Figure 6 shows the test gun barrel containing 32 riflings. Prior to push testing, the as-sprayed rotating band was machined on the lathe to 77.4 mm diameter and 15 mm width, which has a mean surface roughness (R_a) of about 0.5 μm, with a standard deviation of 0.38 μm. For this test, the crosshead speed of the MTS was set at 3 mm s^{-1}, and the required push force as a function of travel was recorded electronically. Prior to and between each test, the gun barrel was cleaned to insure that there were no copper particles stuck inside the barrel. For comparison purposes, a bulk copper rotating band was also prepared for a quasi-static engraving test under the same condition. A cross section of the interaction between the gun barrel and rotating band during the engraving process is schematically shown in Fig. 7.

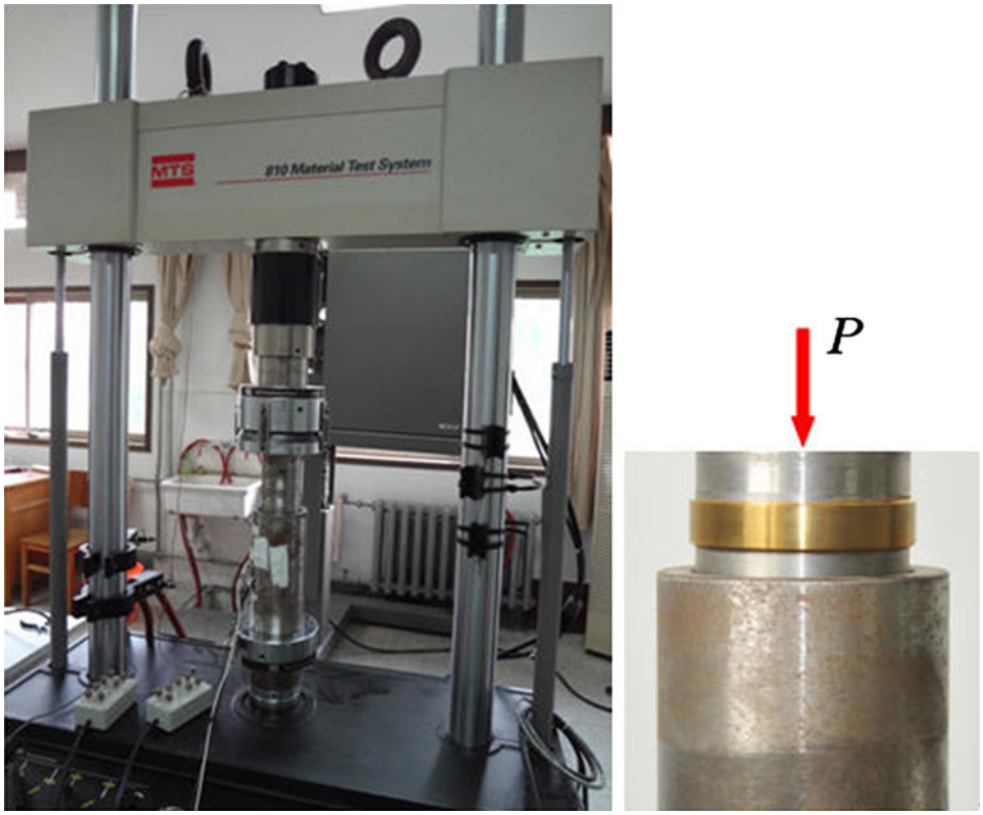

Fig. 5 Quasi-static engraving of rotating band on an MTS 810

3. Results and Discussion

3.1 Coating Microstructures

Figure 8 shows the cross sections of the arc-sprayed aluminum bronze coating. Thick and continuous coatings of aluminum bronze were formed by the HVAS process. The images show that the coatings present a relatively dense structure with low quantity of porosity and cracks and exhibit good adhesion to the substrate. There are few relatively dispersed pores visible in some coatings (as indicated by arrows in Fig. 8(c)). The estimation of the porosity of the coating is about 1.6% by image analysis, with a standard deviation of 0.56%. EDX analyses of points A, B, and C in Fig. 8(c) are shown in Fig. 9. The coating is composed of pure Cu, pure Al, oxides such as CuO, Al_2O_3, etc. It can be seen from Fig. 8(a) and 9 that the bronze plays the role of the binder and the distribution of Al/Al_2O_3 in the bronze matrix is relatively even. During the electric arc spraying, the aerodynamic shear on the droplet surface may enhance the amount of in-flight oxidation by promoting entrainment and mixing of the surface oxide within the droplet (Ref 15); thus, Al_2O_3 is formed on the surface of Al droplets. Formation of Al_2O_3 will prohibit the inside of the aluminum droplets from further oxidation because the Al_2O_3 film is dense and compact. Al droplets enwrapped with Al_2O_3 film can be deemed as reinforced phases (particles) and entrapped by the ductile matrix phase (bronze) and embed into the previously formed deposits.

Fig. 6 A short rifled gun barrel for push testing

Microhardness of the cross section of deposited aluminum bronze coatings has been tested. The hardness of the aluminum bronze coating is around $Hv_{0.025}$ = 120-150, with a standard deviation of 25.98 $Hv_{0.025}$, which is significantly increased compared to pure Cu (about 80 $Hv_{0.025}$). This

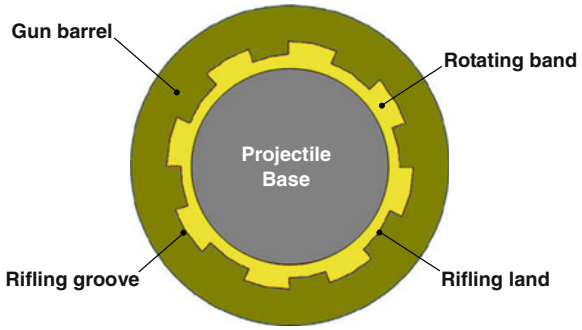

Fig. 7 Cross section of interaction between gun barrel and rotating band

can be mainly attributed to the strong tamping effect of the reinforced phases and the strain-hardening effect as a result of plastic deformation during droplet impacting. Alumina enhances the microhardness of the bronze-alumina composite coatings (Ref 13). In addition, the very low porosity level of coatings contributes to an increase in the hardness of the material (Ref 16).

3.2 Tribological Behavior

Figure 10 shows a representative evolution of the friction coefficient of aluminum bronze coatings versus time under two kinds of test conditions (the former 60 rpm and 700 N, the latter 180 rpm and 1100 N). The friction coefficient of the latter condition is higher than that of the former condition in the beginning of the tests. After a short run-in period (about 400 s), the friction coefficient arrives at a relatively steady state under the former condition, whereas that of the latter condition reaches steady state after an 800-s friction test. It is observed that the friction coefficient of about $\mu = 0.2$-0.3, with a standard deviation of 0.06, is obtained at the end of the test for both conditions. However, the mass loss of aluminum bronze coating under the latter condition is two times higher than that of the former. Comparing the worn surfaces between specimens under low and high load condition, see Fig. 11, the former exhibits slight plastic deformation, while the latter shows larger plastic deformation, plowing, particle delamination, and fragmentation of deposited droplets (particles) and cracks. When large plastic deformation occurs in the contacting surfaces, the two surfaces are prone to stick with each other due to friction heat that is induced by rubbing, thus leading to high friction. For arc-sprayed coatings, the interfaces between the deposited droplets (particles) can be considered weak zones. The tribological behavior of the coating is determined by the dynamic process occurring on the surface layer involved in the frictional process. Under repeated shear forces induced from high load, cracks occurred at these interfaces, and droplets (particles) tend to be smashed by the sliding ring. Figure 11(b) shows a particle that was torn off from the worn surface and may act as a ''third body'' in the following sliding process. A three-body abrasion in the friction process plays an important role in mass loss of the coating. The EDX analyses of worn surfaces under

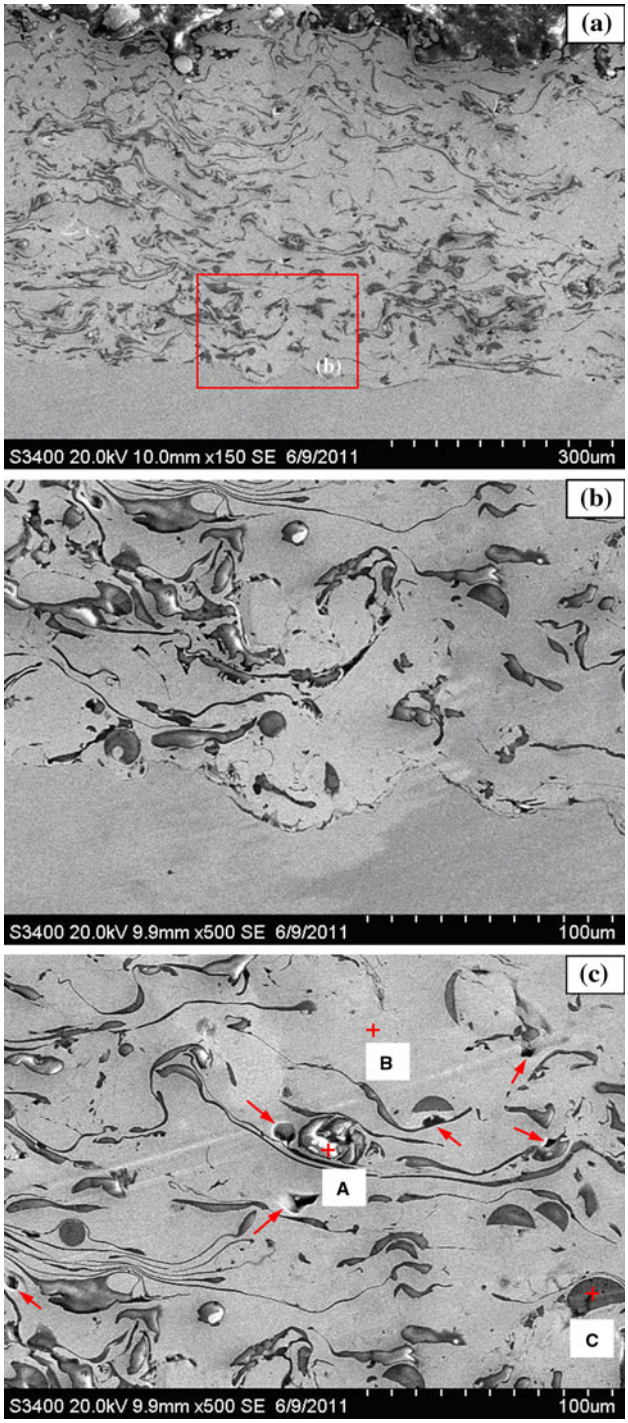

Fig. 8 SEM morphologies of cross-sectional aluminum bronze coating

both conditions showed that they contained Fe, see Fig. 11(c) and (d), which came from the mating surface. No distinct difference for the two coatings was found from the worn surfaces, indicating the same friction coefficient of about 0.25 in steady state.

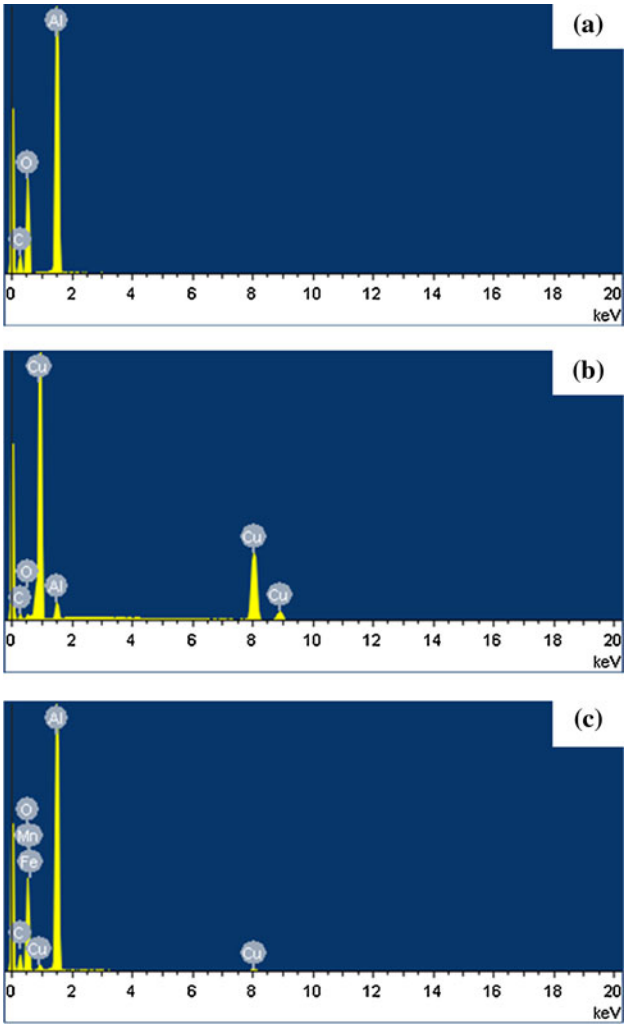

Fig. 9 EDX analysis of point A, B, and C in Fig. 8(c)

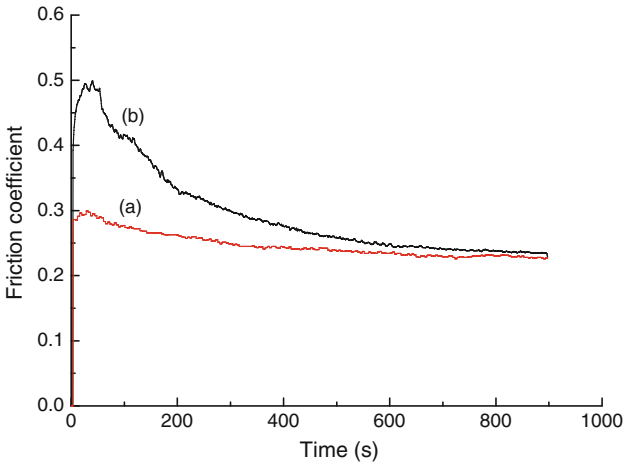

Fig. 10 Friction coefficient evolution for the aluminum bronze coatings: (a) 60 rpm/700 N and (b) 180 rpm/1100 N

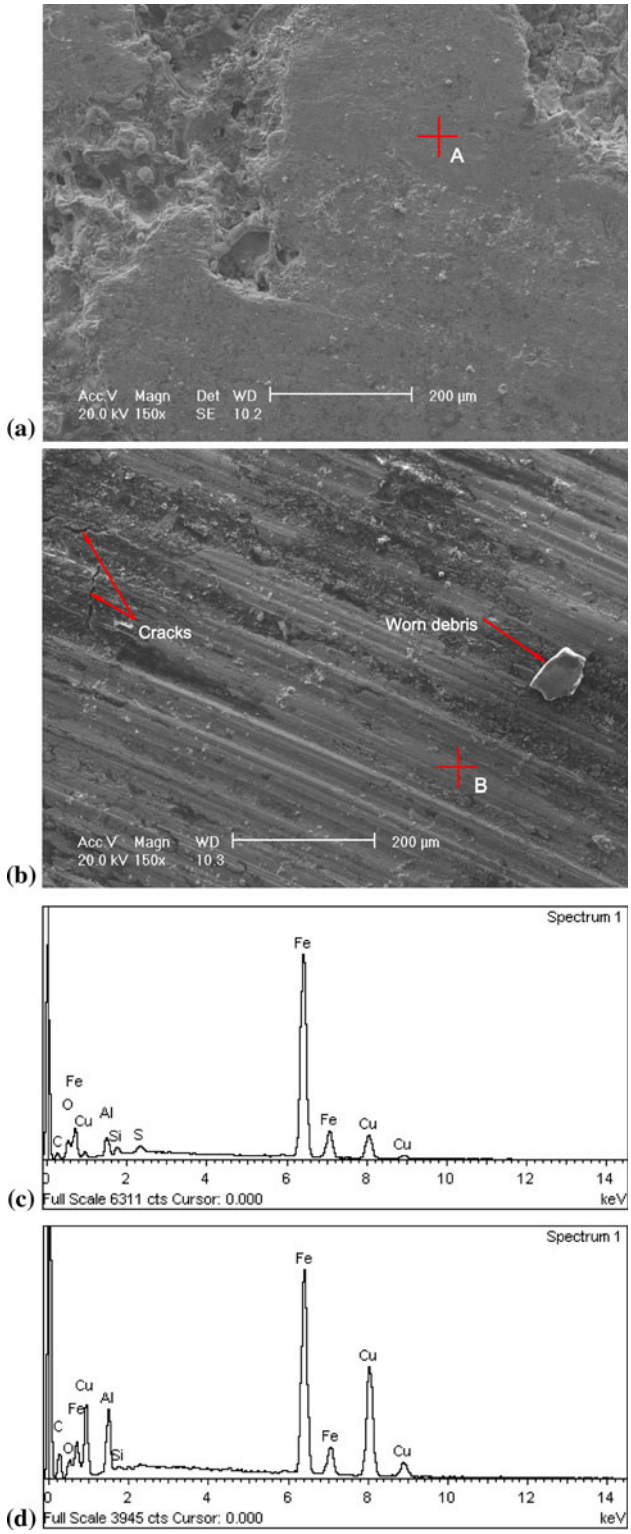

Fig. 11 Wear morphologies of the aluminum bronze coatings: (a) 60 rpm/700 N, (b) 180 rpm/1100 N, (c) EDX analysis of point A, and (d) EDX analysis of point B

3.3 Push Force and Rotating Band Deformation

Figure 12 shows the resulting load versus displacement profiles for the engraving of aluminum bronze rotating band and bulk copper rotating band. It is observed that two load profiles are similar for a given displacement rate. In general, both the profiles have an initial ramp-up in load as the rotating band begins to engrave; some distance of push where the engraved rotating band is located is translated through the barrel. The load eventually falls to zero as the rotating band is pushed completely through the short rifled gun barrel. The load profiles for the different push tests have two distinct peaks. The first peak is just as the rotating band has been completely engraved and the second is right before the projectile exits the rifling. In the present push tests, the first load peak occurred at about 20-mm displacement and the second load peak at about 60 mm, where the rifling ended. For aluminum bronze rotating band, the two load peaks were 138.4 and 131.2 kN, whereas those of the bulk copper rotating band are 180.9 and 163.9 kN. Obviously, the push force of the engraving aluminum bronze rotating band is lower than that of the bulk copper rotating band.

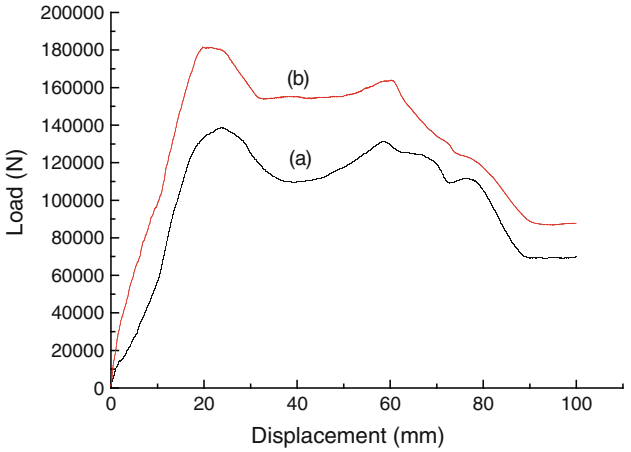

Fig. 12 Load vs. displacement for engraving rotating band with 3-mm/s displacement rate: (a) aluminum bronze and (b) bulk copper

It can be seen from Fig. 8(a) that the aluminum bronze coating was relatively coarse; however, it got low roughness of 0.5 μm after finish machining on a lathe. Figure 13(a) and (b) shows the machined aluminum bronze coating and engraved rotating band, respectively. For reference, the bulk copper rotating band before and after the engraving process is shown in Fig. 13(c) and (d). It is found that the aluminum bronze rotating band has successfully endured the complete engraving process, indicating high bonding strength between the coating and substrate, which is consistent with the interface shown in Fig. 8(a) and (b). A comparison between Fig. 13(b) and (d) indicates that the aluminum bronze rotating band also has good plasticity. No spall of the aluminum bronze coating occurs after the engraving process.

As aforementioned, the hardness of the as-sprayed aluminum bronze coating is higher than that of the bulk copper. However, the push force of engraving the aluminum bronze rotating band is smaller than that of the bulk copper rotating band shown in Fig. 12. The difference of material properties between the as-sprayed aluminum bronze and the bulk copper is responsible for this phenomenon. The ductility of bulk copper is better than that of the as-sprayed aluminum bronze coating, which is confirmed in Fig. 14. For the bulk copper rotating band, copper pushed by the land of the gun barrel is accumulated in the end of the formed groove and does not separate from the rotating band, whereas aluminum bronze coating pushed by the land separates from the rotating band (as indicated by the circle in Fig. 14a and b). The larger deformation of the bulk copper rotating band during the engraving process corresponds to a higher push force.

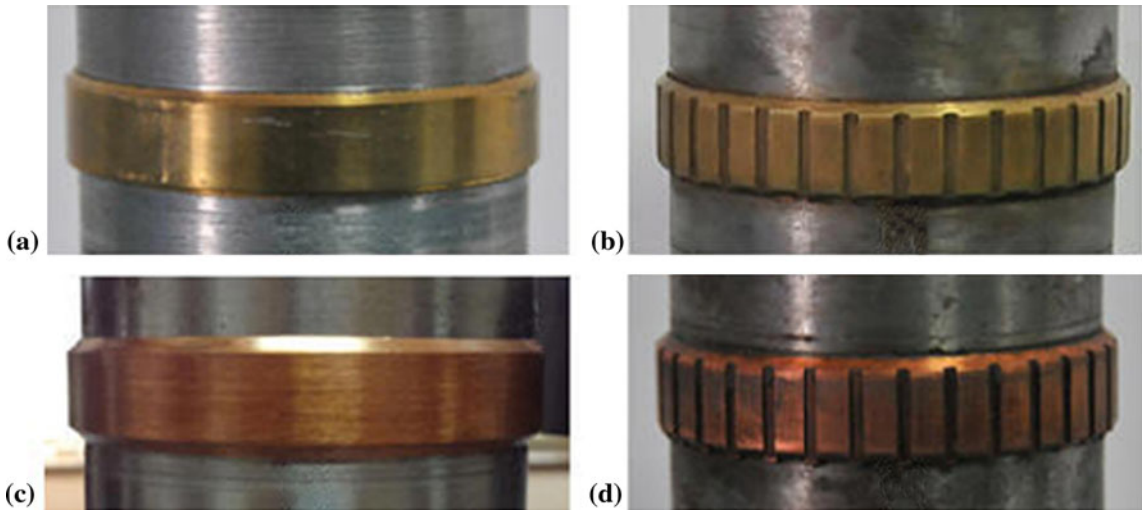

Fig. 13 Rotating band: (a) aluminum bronze before engraving, (b) aluminum bronze engraved, (c) bulk copper before engraving, and (d) bulk copper engraved

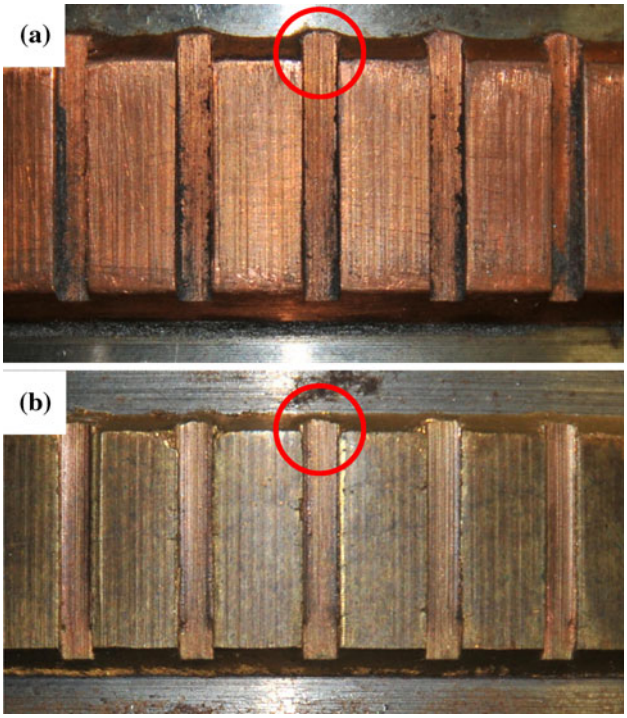

Fig. 14 Deformation of rotating band: (a) bulk copper and (b) aluminum bronze

Cold spray (CS), also termed as cold gas dynamic spray (CGDS) or kinetic spray, is a new member of the thermal spray technologies. The CS process is based on acceleration of small solid particles to a supersonic velocity using compressed and heated gases, generally nitrogen, helium, and air. The adhesion of the particles depends on the plastic and strong deformation they suffer on impingement to the surface. The use of CS has been demonstrated for the production of bulk copper deposits by Gärtner et al. (Ref 17) and Wu et al. (Ref 18). Minnicino et al. (Ref 19) prepared a copper rotating band on an aluminum projectile component using the CS process. Four 155-mm projectiles with a cold-sprayed copper rotating band were fired for demonstration. However, the spall of the copper rotating band at the muzzle exit was found (two instances). Whether the HVAS aluminum bronze rotating band spalls or survives under firing condition will be investigated in our future work.

4. Conclusions

Aluminum bronze coatings were successfully prepared using the HVAS technique. The microstructure, microhardness, and tribological behavior of the as-sprayed coatings were characterized. Quasi-static push tests for engraving of rotating bands made of as-sprayed aluminum bronze coating and bulk copper were conducted. Based on the results in this study, the following conclusions can be drawn:

1. The porosity of the as-sprayed aluminum bronze coatings is about 1.6%. The as-sprayed coatings present a dense microstructure and exhibit a higher microhardness than that of the bulk copper, which may be ascribed to the effects of strong tamping and strain hardening of the hard reinforced phases Al/Al_2O_3 during the impacting process.
2. The as-sprayed coatings present friction coefficient of about 0.2-0.3 in steady state under dry sliding friction test conditions. Plastic deformation and adhesion between the two sliding pairs play significant roles on the tribological behavior. Moreover, particle delamination, plowing, and fragmentation of deposited droplets occurred under high loading.
3. The quasi-static push test results showed that the as-sprayed coatings present high bonding strength and have good plasticity. The push force of the engraving bulk copper rotating band is higher than that of the aluminum bronze, which is due to the larger plastic deformation. The difference of the mechanical properties between the two materials is mainly responsible for this phenomenon.
4. The aluminum bronze coating prepared by the HVAS process should be a good candidate for application to a rotating band of large-caliber projectiles. Optimization of process parameters (voltage, current, air pressure, and spray distance) and aluminum bronze wire composition will improve the as-sprayed coating properties to fully meet the demands of modern large-caliber guns.

Acknowledgments

The authors are grateful for financial support from the Natural Science Foundation of China (51175512). They would also like to acknowledge the valuable contributions made by Dr. Xiang-gui Ni.

References

1. R.S. Montgomery, Interaction of copper-containing rotating band metal with gun bores at the environment present in a gun tube, *Wear*, 1975, **33**, p 109-128
2. R.S. Montgomery, Friction and wear at high sliding speeds, *Wear*, 1976, **36**, p 275-298
3. R.S. Montgomery, Surface melting of rotating bands, *Wear*, 1976, **38**, p 235-243
4. R.S. Montgomery, Projectile lubrication by melting rotating bands, *Wear*, 1976, **39**, p 181-183
5. R.S. Montgomery, Wear of projectile rotating bands, *Wear*, 1985, **101**, p 347-356
6. T. Matsuyama. Friction and wear mechanism at high sliding speeds. *19th International Symposium of Ballistics*, 2001
7. M. Lisov, Modeling wear mechanism of artillery projectiles rotating band using variable parameters of internal ballistic process, *Sci. Tech. Rev.*, 2006, **LVI**(2), p 11-16
8. M. Schupfer, K. Steinhoff, R. Röthlisberger. New materials for large-caliber rotating bands for high charges. *19th International Symposium of Ballistics*, 2001

9. G. Akdogan, T.A. Stolarski, and S. Tobe, Surface fatigue of molybdenum and Al-bronze coatings in unlubricated rolling/sliding contact, *Wear*, 2002, **253**, p 319-330
10. Z. Zhang, D. Li, and S. Wang, High temperature performance of arc-sprayed aluminum bronze coatings for steel, *Trans. Nonferr. Met. Soc. China*, 2006, **16**, p 868-872
11. S. Alam, S. Sasaki, and H. Shimura, Friction and wear characteristics of aluminum bronze coatings on steel substrates sprayed by a low pressure plasma technique, *Wear*, 2001, **248**, p 75-81
12. K.S. Tan, R.J.K. Wood, and K.R. Stokes, The slurry erosion behaviour of high velocity oxy-fuel (HVOF) sprayed aluminum bronze coatings, *Wear*, 2003, **255**, p 195-205
13. J.M. Miguel, J.M. Guilemany, and S. Dosta, Effect of the spraying process on the microstructure and tribological properties of bronze-alumina composite coatings, *Surf. Coat. Technol.*, 2010, **205**, p 2184-2190
14. K. Cooke, G. Oliver, V. Buchanan, and N. Palmer, Optimisation of the electric wire arc-spraying process for improved wear resistance of sugar mill roller shells, *Surf. Coat. Technol.*, 2007, **202**, p 185-188
15. D. Guillen, B.G. Williams, *Thermal Spray Connects: Explore its Surface Potential*, E. Lugscheider, Ed., DVS, Düsseldor, DE, 2005, pp. 1150-1154
16. S.H. Zahiri, C.J. Antonio, and M. Jahedi, Elimination of porosity in directly fabricated titanium via cold gas dynamic spraying, *J. Mater. Process. Technol.*, 2009, **209**, p 922-929
17. F. Gärtner, T. Stoltenhoff, T. Schmidt, and H. Kreye, The cold spray process and its potential for industrial application, *J. Therm. Spray Technol.*, 2006, **15**(2), p 223-232
18. X.K. Wu, J.S. Zhang, X.L. Zhou, H. Cui, and J.C. Liu, Advanced cold spray technology: deposition characteristics and potential applications, *J. Therm. Spray Technol.*, 2012, **55**(2), p 357-368
19. M. Minnicino, M. Trexler, V. Champagne, A new method for fabricating copper rotating bands on munitions. *Proceedings of the 44th Annual Gun and Missile Systems Conference and Exhibition*, April 6-9, 2009 (Kansas City, MO, USA)